General Behavior of Braced Excavation in Bukit Timah Granite Residual Soils: a Case Study

Wengang Zhang[abc*,a] *Researcher, Key Laboratory of New Technology for Construction of Cities in Mountain Area (Chongqing University), Ministry of Education, Chongqing 400045, China;* [b] *Professor, School of Civil Engineering, Chongqing University, Chongqing 400045, China;* [c] *Research Fellow, School of CEE, Nanyang Technological University, 639798 Singapore; email: zhangwg@ntu.edu.sg*

Anthony Teck Chee Goh, *Associate Professor, School of CEE, Nanyang Technological University, Singapore; email: ctcgoh@ntu.edu.sg*

ABSTRACT: *The excavation system performance and ground movement behavior for the cut-and-cover excavation for the Downtown Line 2 Cashew Station in Singapore is presented. The information presented includes ground settlement profiles, wall deflection profiles, strut loads, and ground water monitoring behavior. Construction activities and remedial measures that were undertaken are also presented. Comparisons of the measured wall deflections and the ground surface settlements are also performed against the empirical methods/charts from the literature. It is hoped that this case study will provide useful reference and insights for future projects involving excavation in the Bukit Timah Granite residual soils.*

KEYWORDS: braced excavation, Bukit Timah Granite residual soil, wall deflection, ground settlement, strut force, piezometric level

SITE LOCATION: IJGCH-database.kmz (requires Google Earth)

INTRODUCTION

Contract C913 of Downtown Line 2 (DTL2) involves construction of stations at Hillview in the south, and Cashew in the middle, twin bored tunnels between Hillview and Cashew, and twin bored tunnels between Cashew and the Cross-over box of C912 in the north. The Cashew station is about 225 m long and up to about 60 m wide with the formation levels around 95.5 mRL (meter Reference Level), constructed by the cut-and-cover method. Figure 1 provides an overview of the station location.

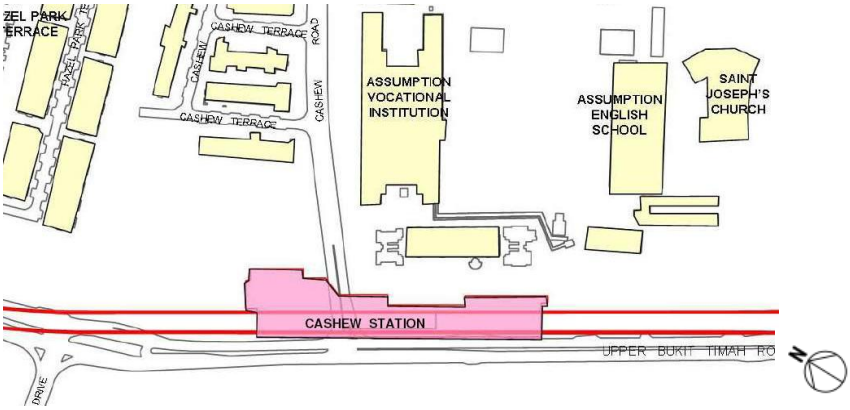


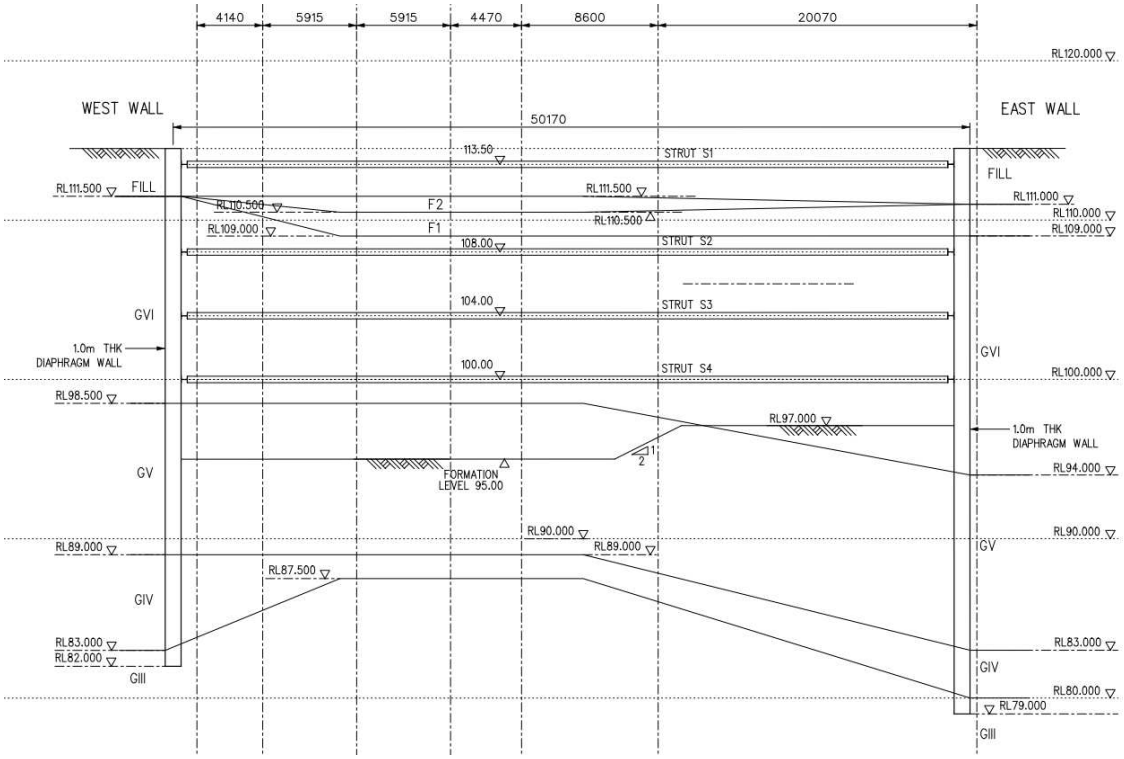
Figure 1. Location of Cashew Station.

Submitted: 05 November 2015; Published: 10 October 2016
Reference: Zhang, W., and Goh, A. T. C. (2016). *General Behavior of Braced Excavation in Bukit Timah Granite Residual Soils: a Case Study*. International Journal of Geoengineering Case histories, http://casehistories.geoengineer.org, Vol.3, Issue 3, p.190-202. doi: 10.4417/IJGCH-03-03-05

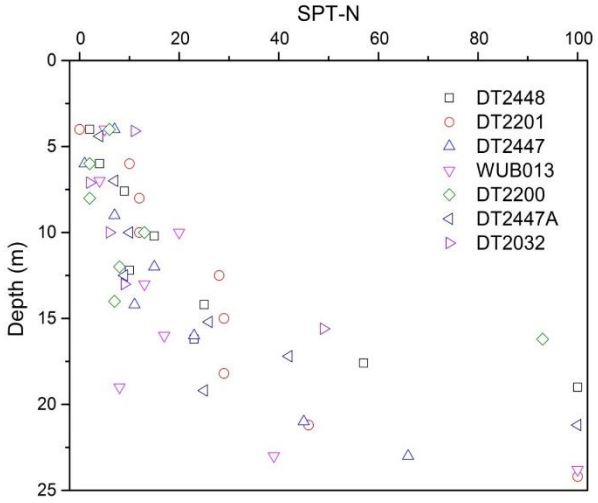
GENERAL PROJECT DESCRIPTION

Subsurface Conditions

Based on the geological data, the ground conditions comprise of Fill, Kallang Formation, residual soil, completely weathered materials, highly weathered materials and moderately weathered to fresh rock. Figure 2a shows the cross-sectional view and the soil profiles based on existing boreholes. This figure presents the typical geologic units, the generalized site stratigraphy and the relative position between each strut level and geologic unit. Figure 2b summarizes the variation of SPT-N values with depth based on a number of borelogs.



(a)



(b)

Figure 2. Cashew station subsurface conditions:
(a) geological soil profiles and cross-sectional view; (b) SPT-N variation with depth.

Excavation Support System Description

The Earth Retaining Support System (ERSS) comprised of 1 m thick diaphragm walls with 4 layers of HY 700 struts. Double waler beam HY700 with bracket HY400 is used. The average wall length is 25 m. The struts are preloaded to 100% of design load ranging from 100 to 350 kN/m (1st level: 100 kN/m, 2nd level: 300 kN/m, 3rd and 4th level: 350 kN/m). Figure 3 shows the typical strutting arrangement plan. To provide a hydraulic cut-off within the rock mass, fissure grouting was carried out at zones outside the excavation down to an adequate depth below the excavation base level. In addition, the recharging wells were installed behind the excavation areas that are sensitive to settlements.

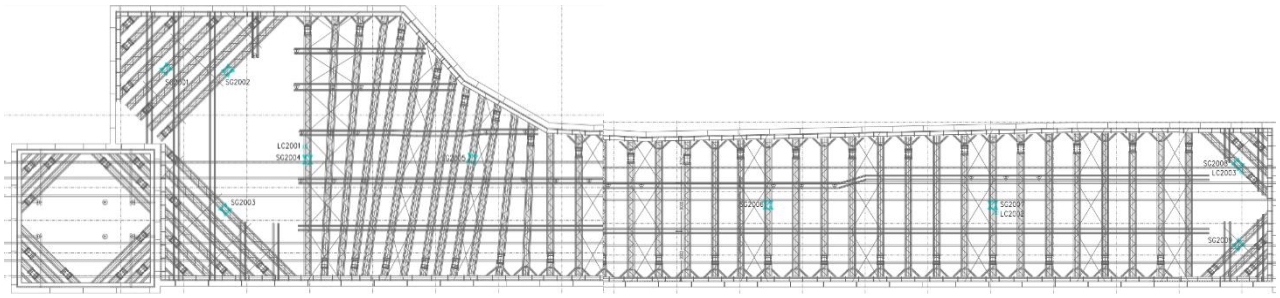


Figure 3. Typical strutting arrangement plan.

Construction Activities

The main excavation and construction activities and the corresponding dates together with the construction day numbers are summarized in Table 1. Construction day number 1 denotes the day of June 3rd, 2011, corresponding to the beginning of the excavation of the first level soil at the project site. The construction days correspond to the calendar days and advance sequentially until the end of construction. Construction days include weekends and public holidays. Construction activities at the site are separated into three distinct stages: Stage 1 - wall installation and fissure grouting, denoted as P; Stage 2 - support system installation and excavation; and Stage 3 - strut removal and backfill. The actual beginning and duration of each stage slightly differs depending on the location within the excavation.

Table 1. Days of significant excavation and construction activity.

Activities		Dates (Construction days)
P	construction of the diaphragm walls	19-06-2010 to 17-06-2011 (-348 ~ 15)
	fissure grouting	17-08-2010 to 30-07-2011 (-289 ~ 58)
S1	excavation of the 1st level soil	06-06-2011 to 15-09-2011 (4 ~ 105)
	installation of level 1 strut	09-06-2011 to 15-11-2011 (7 ~ 166)
S2	excavation of the 2nd level soil	02-09-2011 to 20-11-2011 (92 ~ 171)
	installation of level 2 strut	24-09-2011 to 16-12 2011 (114 ~ 197)
S3	excavation of the 3rd level soil	09-12-2011 to 31-12-2011 (190 ~ 212)
	installation of level 3 strut	16-12-2011 to 10-02-2012 (197 ~ 253)
S4	excavation of the 4th level soil	20-01-2012 to 24-02-2012 (232 ~ 267)
	installation of level 4 strut	1-02-2012 to 24-03-2012 (244 ~ 296)
S5	excavate to final excavation level FEL	23-02-2012 to 29-05-2012 (266 ~ 362)
R1	removal of strut level 4	15/5/2012 to 16/8/2012 (345 ~ 441)
R2	removal of strut level 3	27/8/2012 to 18/3/2013 (452 ~ 655)
R3	removal of strut level 2	10/11/2012 to 18/3/2013 (527 ~ 655)
R4	removal of strut level 1	30/1/2013 to 28/6/2013 (608 ~ 757)

Field Instrumentation

Monitoring data collected during the construction included diaphragm wall deflections (using in-wall inclinometers), pore water pressures (using vibrating wire piezometers), ground settlements and strut loadings. Data from the inclinometers and piezometers were obtained daily during wall installation and excavation, and at least on a weekly basis after the excavation

had reached its final depth. Strut loads were determined from strain gauges or load cells, carried out daily during excavation, and weekly after the excavation was completed. Figure 4 shows a plan view of the Cashew station instrumentation layout including the instrument types and locations. Notations of the symbols are as follows: I - inclinometer; GWV - vibrating wire piezometer; LG - ground settlement marker; SG - strain gauge and LC - load cell.

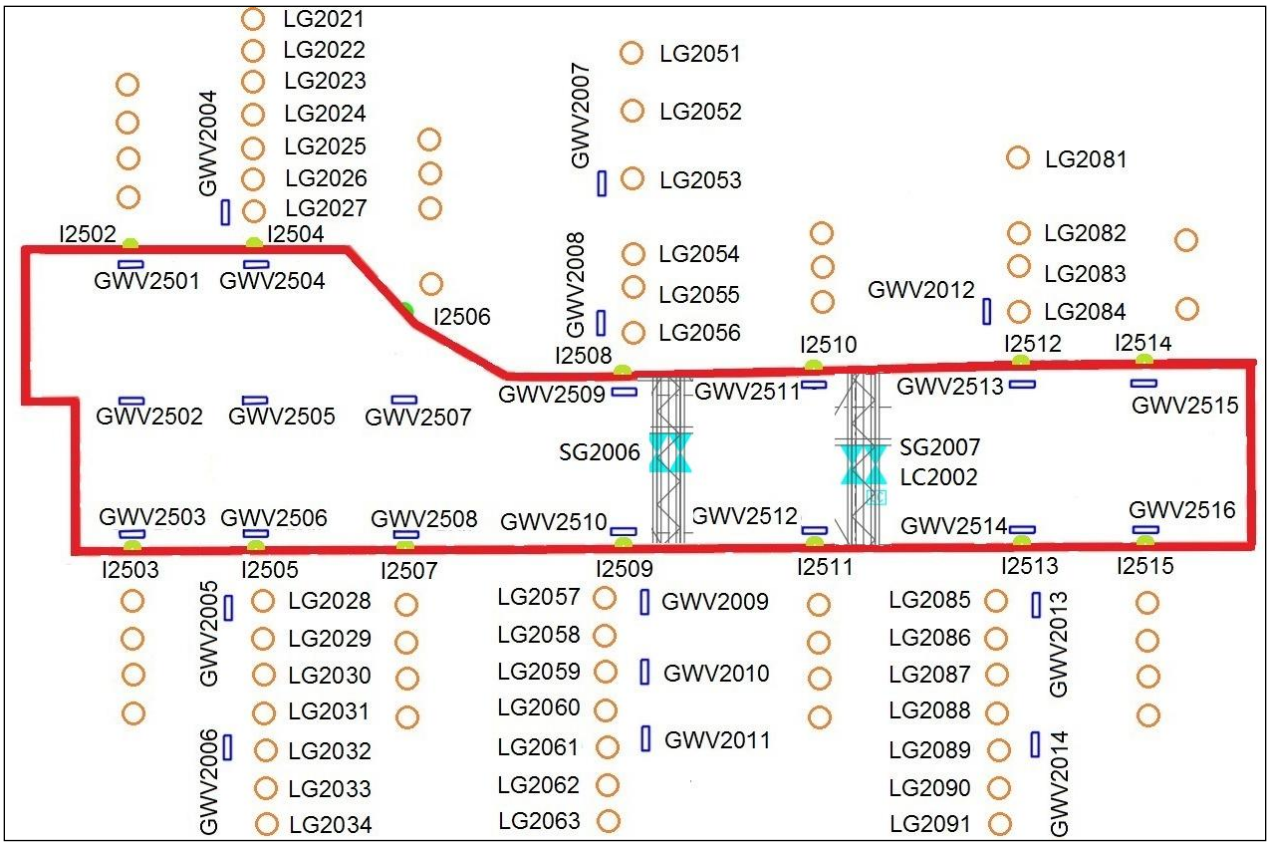


Figure 4. Cashew station instrumentation layout.

PERFORMANCE AND OBSERVED BEHAVIOUR OF FIELD INSTRUMENTATION

Field instrumentation responses including lateral wall deformations, ground settlements, pore water pressures, and strut loadings are presented and related to construction activities. For brevity, only some typical cross-sections are reported. Cross-sections are named after the inclinometer number (for example section 2 for inclinometer I2502), as shown in Figure 4.

Lateral Wall Movements and Ground Settlement

Section 8 is in the middle part of the east wall. The instrumentation consists of in-wall inclinometer I2508 and ground settlement markers from LG2051 to LG2056. These ground settlement markers are 96 m, 81 m, 66 m, 21 m, 18 m and 3 m away from the excavation, respectively. Figure 5 shows the lateral response for inclinometer I2508 and the corresponding ground settlement. Note the cantilever shape of the deformation curve for "excavate and install S2" becomes concave at the following stage (excavate and install S3) possibly because of the restraint from the 2nd level strut. Figure 5 shows that the maximum lateral wall deflection at the end of excavation was approximately 9.0 mm. The maximum ground settlement at the end of excavation was about 87.0 mm.

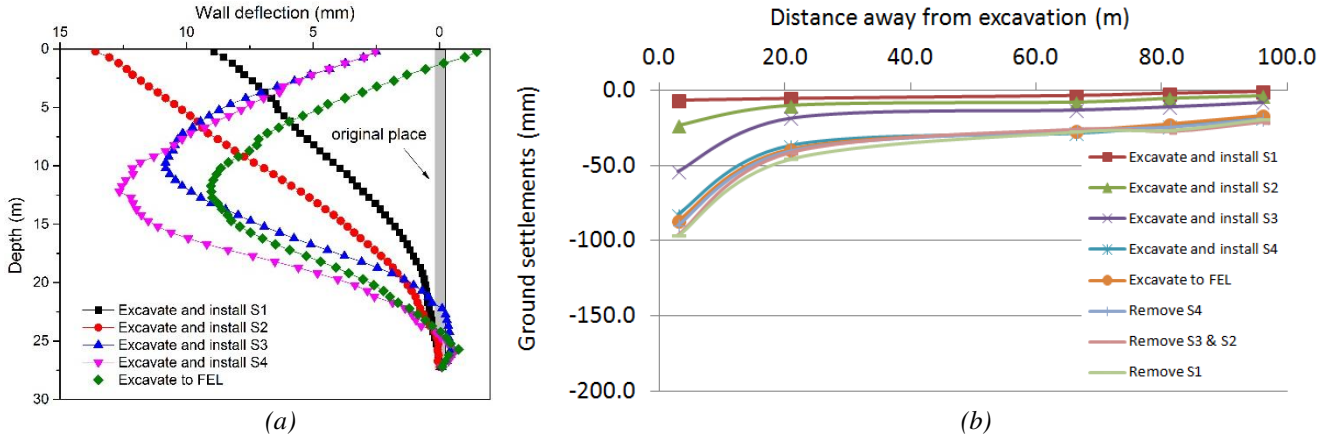


Figure 5. Lateral response for inclinometer I2508 and the ground settlement for section 8: (a) Lateral wall deflections; (b) Ground settlements.

Section 9 is in the middle part of the western wall. The instrumentation consists of in-wall inclinometer I2509 and seven ground settlement markers from LG2057 to LG2063. These ground settlement markers are 6 m, 11 m, 23 m, 29 m, 34 m and 49 m away from the excavation, respectively. Figure 6 shows the lateral response for inclinometer I2509 and the corresponding ground settlement. Note that the deformation curve shape for "excavate and install S2" is cantilever and changes to concave shape on the following stage. The general trend is for the ground settlement to increase with increasing excavation and to decrease with distance from the excavation. There is minimal ground settlement at distances greater than 50 m from the wall. Figure 6 shows that the maximum lateral wall deflection at the end of excavation was approximately 17.1 mm. The maximum ground settlement was about 118.3 mm.

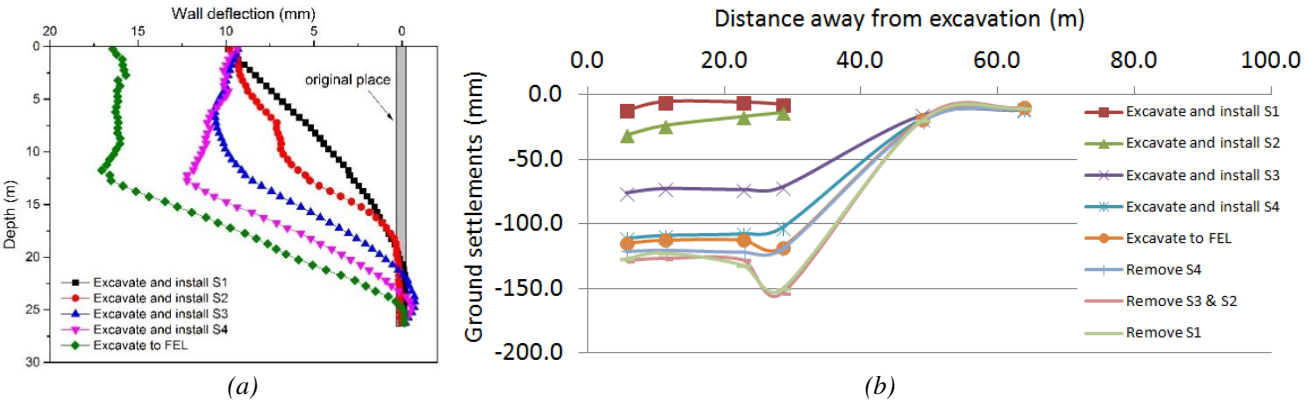
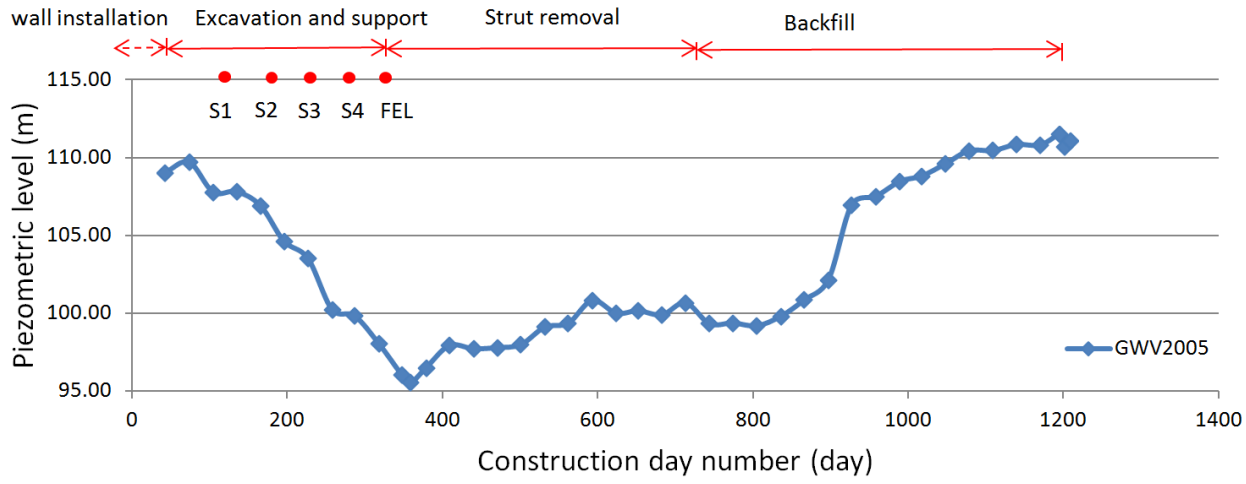


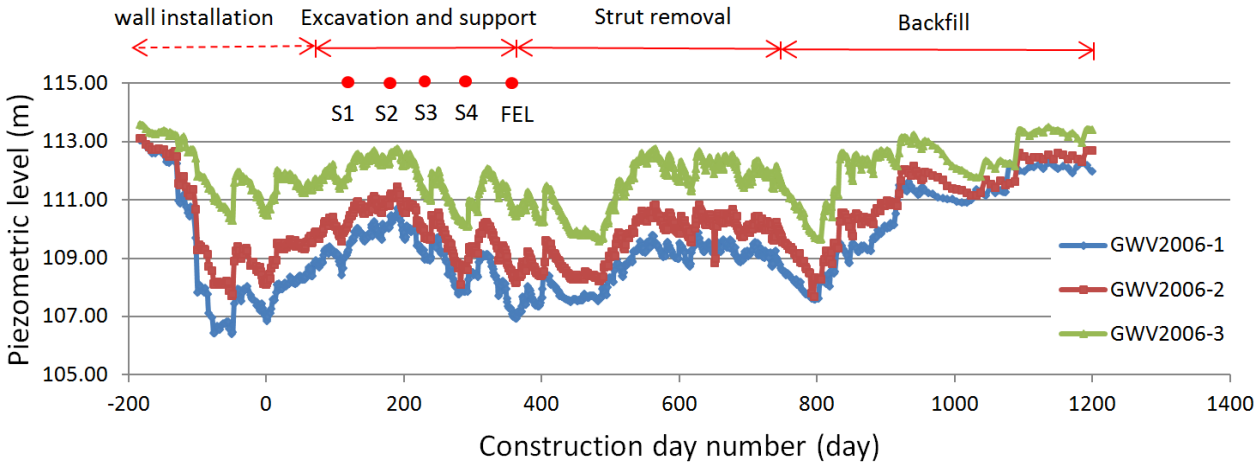
Figure 6. Lateral response for inclinometer I2509 and the ground settlement for section 9: (a) Lateral wall deflections; (b) Ground settlements.

Pore Water Pressure Response

As indicated in Figure 4, piezometers were installed inside and outside the excavation areas. This section mainly presents the piezometric level changes outside the excavation since the groundwater drawdown is likely to have influenced the ground settlements. For brevity, only Piezometers GWV2005 and GWV2006 are reported here. Piezometers GWV2005 and GWV2006 are in the same section as inclinometer I2506. Piezometer GWV2005 was located 6 m from the diaphragm wall whereas GWV2006 was located 34 m from the wall. Figure 7 shows the piezometric level changes of GWV2005 and GWV2006. Installation depths of GWV2006-1, GWV2006-2 and GWV2006-3 are 29.0 m, 15.0 m and 7.0 m, respectively. It should be noted that for GWV2005, most of the groundwater drawdown occurs when excavation proceeded to the final excavation level FEL.



(a)



(b)

Figure 7. Piezometric level changes of: (a) GWV2005; and (b) GWV2006.

Strut Forces

Figure 4 sketches two sets of instrumented struts S2006 and S2007, and they were used to measure strut forces with excavation. Each set consists of four instrumented levels. For S2007 level 1 (strut S2007-1), strut forces were derived from both strain gauge and load cell readings were obtained for comparison. Figure 8 shows the measured strut forces from the strain gauges with construction day numbers for S2006 and S2007. After reaching a peak following excavation to the 1st stage, loads for the 1st strut level decreased for subsequent excavation stages. Strut loads for the 2nd level remained relatively constant after excavation to 3rd level, while loads recorded at 3rd and 4th strut levels continued increasing to the final excavation level. The removal of strut 4 caused significant increase of the force in strut 3, but minimal changes to the force in struts 1 and 2. Similarly, the removal of strut 2 resulted in significant increase in the force in strut 2. Likewise, the removal of strut 2 caused significant increase in the force in strut level 1.

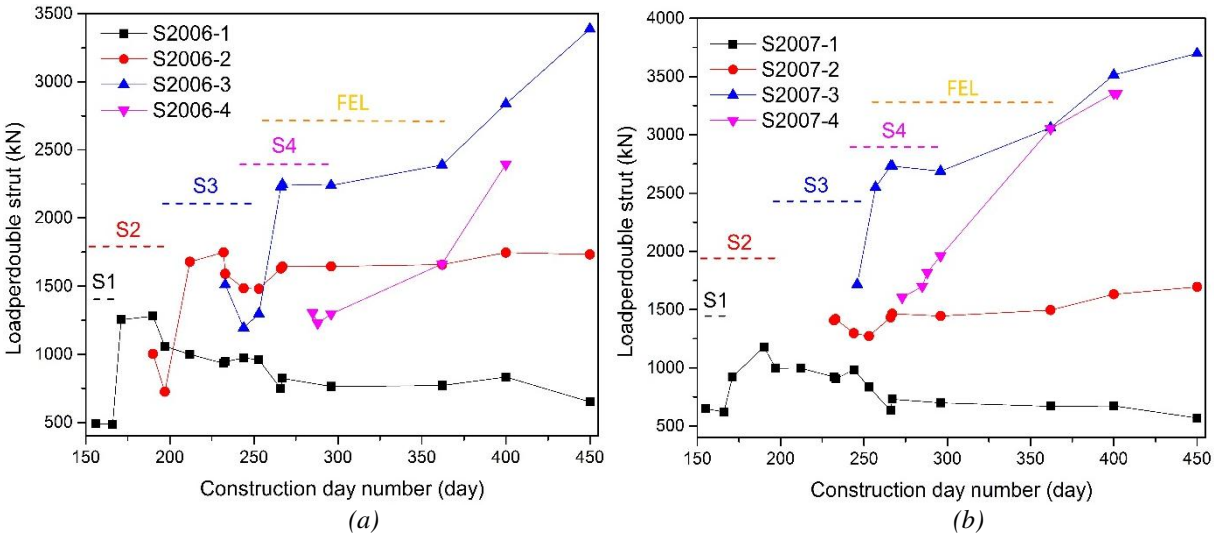


Figure 8. Measured strut forces for: (a) S2006; and (b) S2007.

Figure 9 compares measured strut force SG2007-1 from strain gauges and load cells. Strut loads derived from load cells were generally lower than those from strain gauges. This could possibly be due to errors in strain gauge calibration or because load cells are not as sensitive to temperature changes.

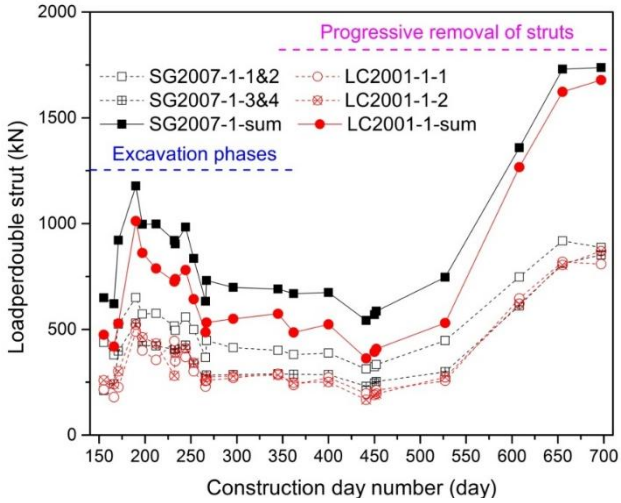


Figure 9. Comparison of SG2007-1 strut force derived from strain gauges and load cells.

Table 2 summarizes the maximum total loads of each strut level for S2006 and S2007 during excavation and after strut removal. Based on these maximum loads and the locations of each level strut, using the tributary area method proposed by Terzaghi and Peck (1967), apparent earth pressure diagrams (APD) have been developed for Bukit Timah Granite residual soils, as shown in Figure 10.

Table 2. Maximum loadings for S2006 and S2007 struts.

Strut No.	Max. loads (kN)	Strut No.	Max. loads (kN)
S2006-1	1593	S2007-1	1738
S2006-2	3517	S2007-2	3477
S2006-3	3403	S2007-3	3699
S2006-4	2396	S2007-4	3357

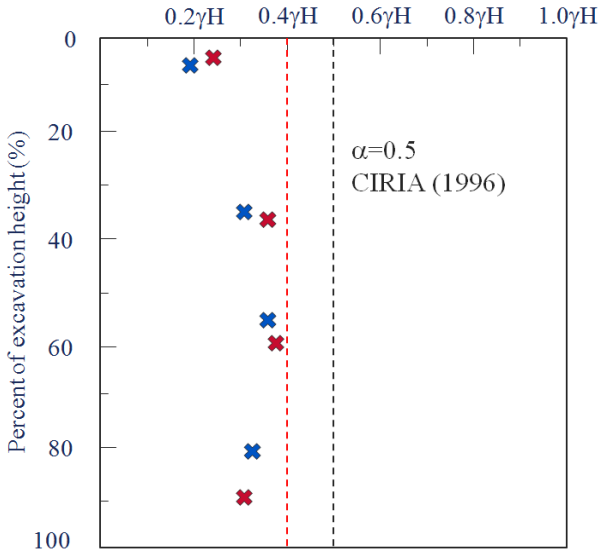


Figure 10. APD developed for Bukit Timah granite residual soils.

OVERALL PERFORMANCE

Table 3 summarizes maximum wall deflection, maximum ground settlement, and maximum groundwater drawdown for each cross-section during and after excavation. Also listed in Table 3 is the diaphragm wall installation depth and final excavation depth for each section. Table 5 lists the normalized maximum wall deflection (defined as the ratio of maximum wall deflection to the final excavation depth) for each section during the strut removal and backfill stages. It can be observed that even though in many cases the maximum wall deflection increased significantly during strut removal, compared with the values at the end of excavation, the normalized maximum wall deflection values were still below 0.2%, with average value of approximately 0.12%. Figure 11 shows the effects of recharging (recharging wells are denoted by the green solid circles) on the maximum ground settlements, denoted by the numbers in red color (unit: mm). For most of the cross-sections where recharging was carried out, the maximum ground settlements are about half of that without recharging.

Table 3. Summary of ground and wall movements with water drawdown for Cashew station.

Section	Wall depth (m)	Final excavation depth (m)	Max. water drawdown (m)	End of excavation		Strut removal and backfill	
				Max. wall deflection (mm)	Max. ground settlement (mm)	Max. wall deflection (mm)	Max. ground settlement (mm)
2	35.5	19.1	—	11.0	40.5	24.4	57.0
3	28.3	19.3	—	14.9	35.1	41.0	54.1
4	36.2	19.2	15.7	13.9	42.0	25.0	56.3
5	31.0	19.3	15.9	13.4	27.7	30.0	34.7
6	36.8	19.2	—	5.5	30.2	18.5	44.0
7	31.5	19.4	—	6.1	48.5	21.4	62.9
8	26.7	19.4	13.5	9.0	87.0	16.7	105.3
9	25.7	19.5	13.6	17.1	118.3	32.1	165.4
10	22.4	19.5	—	7.4	30.7	8.5	43.0
11	26.8	19.9	—	16.5	70.8	31.3	92.6
12	22.9	19.2	14.9	10.4	38.9	17.6	48.4
13	30.4	20.1	13.1	12.5	71.7	24.6	95.6
14	29.5	19.3	—	13.7	25.1	25.8	35.3
15	25.8	20.1	—	8.8	72.2	14.8	98.8

Table 4. Normalized maximum wall deflection depth during strut removal and backfill stage.

Section No.	Normalized maximum wall deflection (%)	Section No.	Normalized maximum wall deflection (%)	Section No.	Normalized maximum wall deflection (%)
2	0.13	7	0.11	12	0.09
3	0.21	8	0.09	13	0.12
4	0.13	9	0.16	14	0.13
5	0.16	10	0.04	15	0.07
6	0.10	11	0.16	Average = 0.12%	

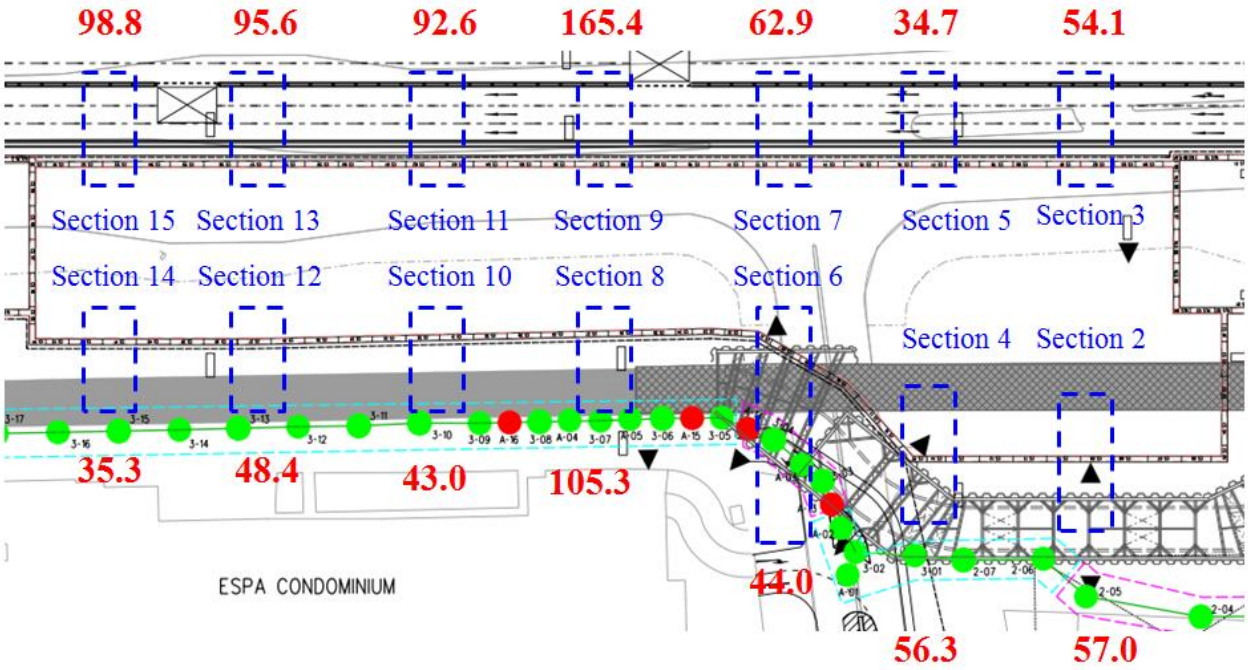


Figure 11. Effect of recharging on ground settlements.

COMPARISON OF MEASURED WALL DEFLECTION AND GROUND SETTLEMENT PROFILES WITH EMPIRICAL METHODS FROM THE LITERATURE

Comparison of Measured Wall Deflection with Empirical Methods from The Literature

Figure 12a and 12b present the maximum wall deflection and the normalized maximum wall deflection (i.e. ratio of maximum wall deflection to the excavation depth) for each excavation stage, respectively. These results show that from the excavation of the second layer soil onwards, the normalized maximum wall deflection was below 0.2%, which is usually adopted as the lower bound by Ou et al. (1993), indicating generally small deflections.

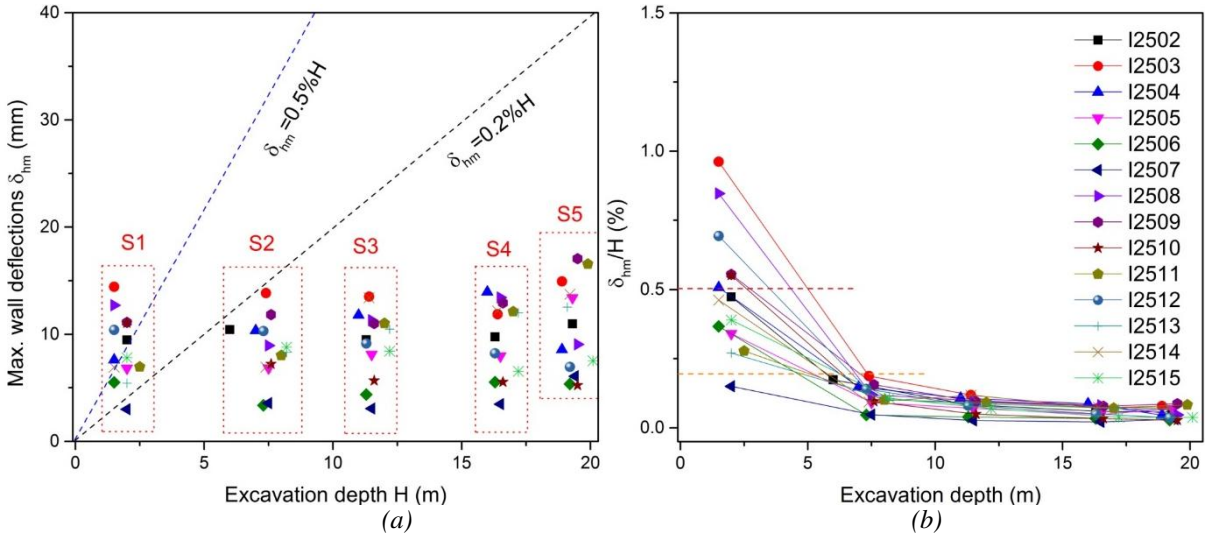


Figure 12. Comparison of wall deflection: (a) Maximum wall deflection versus excavation depth; (b) Ratio of normalized maximum wall deflection versus excavation depth.

Figure 13a presents a chart relating system stiffness and basal stability to maximum normalized horizontal displacements by Clough and O' Rourke (1990). Within the figure, the Cashew case is denoted as a red dot. The system stiffness values for Cashew cross-sections are 261 and the derived Factor of safety values against basal heave are all greater than 4. Figure 13b indicates that the normalized wall deflections at the end of the excavation are even below 0.1%. Generally speaking, the excavation is in the safe side with small wall movements.

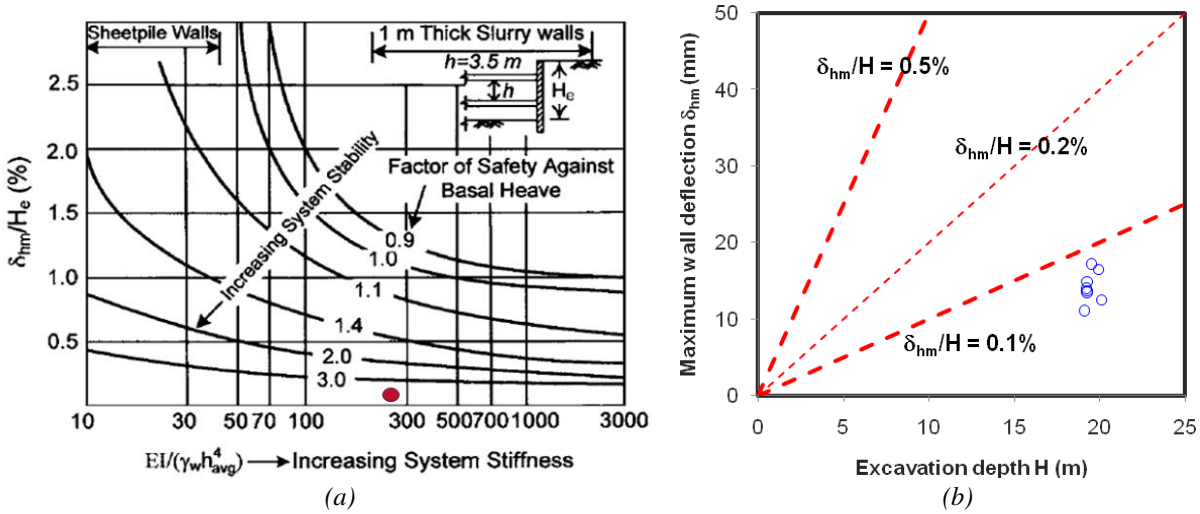
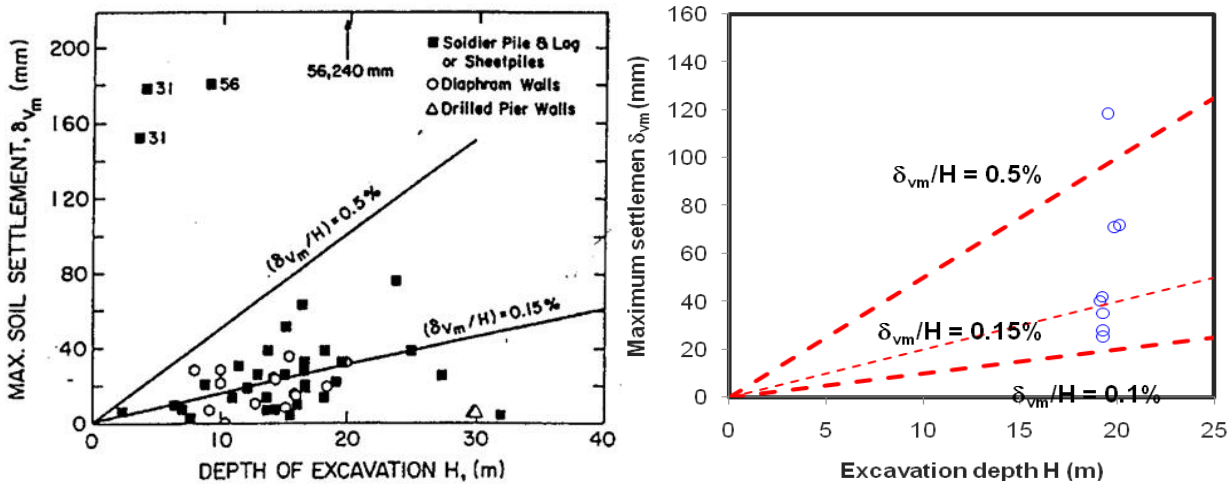


Figure 13. Comparison of wall movement with Clough and O' Rourke 1990 (Figure adapted from Clough and O'Rourke 1990).

Comparison of Ground Settlement Profiles with Empirical Methods from The Literature

Clough and O'Rourke (1990) also related the maximum ground surface settlement measured at the end of excavation with the excavation depth, for walls of varying stiffness in stiff clays, residual soils and sands (Figure 14a). Figure 14b plots the maximum surface settlement values against the 0.5% and 0.15% lines, indicating that the settlement data of Cashew station is slightly greater than cases of similar excavation depth in Clough and O'Rourke's chart, for diaphragm walls, which is attributed to the significant groundwater drawdown.



(a) *(b)*

Figure 14. Comparison of maximum surface settlement with Clough and O' Rourke 1990 (Figure from Clough and O'Rourke 1990).

Based on measured ground settlements until the end of excavation, observed settlement profiles for the fourteen cross-sections were plotted and compared with the concave settlement profile proposed by Hsieh and Ou (1998), as shown in Figure 15. From Figure 15, it is obvious that measured ground settlement profiles at Cashew Station in many sections differed significantly from the concave settlement profile proposed by Hsieh and Ou (1998) and the settlement trough moves outwards as a result of significant groundwater drawdown.

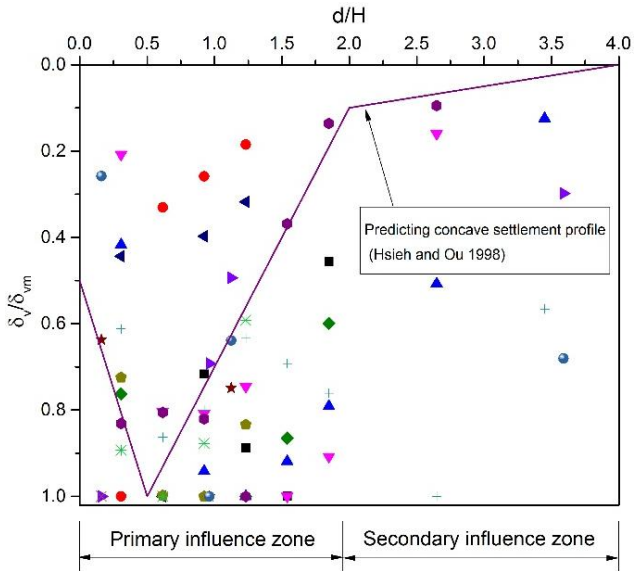
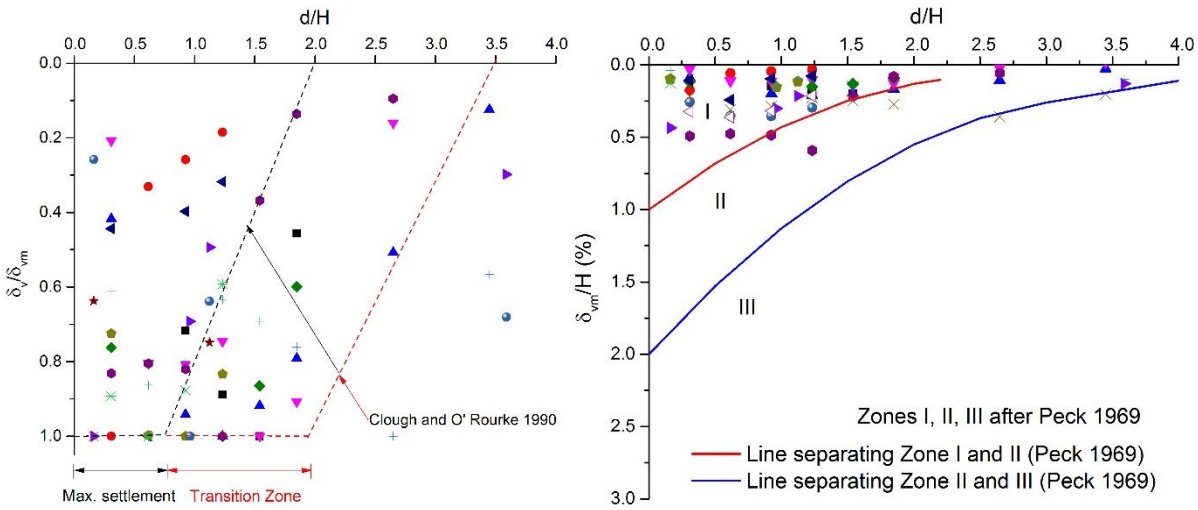


Figure 15. Comparison of ground settlement profiles against Concave settlement by Hiseh and Ou 1998.

Figure 16a plots the ground settlement profiles against the pattern suggested by Clough and O'Rourke (1990). It is obvious that the results are scattered. In addition, for several cross-sections, the maximum ground settlements occurs in the transition zone, indicating that the settlement trough is even wider than estimated by Clough and O'Rourke (1990). However, when the data points are plotted in the pattern suggested by Peck (1969), as shown in Figure 16b, a relatively well-defined grouping of the data can be observed.



(a) *(b)*

Figure 16. Comparison of ground settlement profiles against: (a) Clough and O' Rourke 1990; and (b) Settlement pattern by Peck 1969.

Cham and Goh (2011) proposed a semi-empirical model based on the measured database recorded from the Singapore Mass Rapid Transit Circle Line excavation sites, expressed as below:

$$\delta_v = \delta_{vm} e^{-\frac{(X - X_{\delta vm})^2}{1.2 X_{\delta vm}^2}} \quad (1)$$

in which X = distance from the wall (m); δ_v =ground settlement at the distance X , in mm; δ_{vm} = maximum ground settlement (mm) and $X_{\delta vm}$ =distance from the wall to point of maximum ground settlement (m).

Figure 17 plots the normalized ground settlement profiles observed for the Cashew cross-sections, where the ground surface settlement is normalized by dividing by the maximum surface settlements and the distance behind the excavation was normalized by dividing the distance behind the excavation coinciding with the maximum settlement. From Figure 17, it is obvious that the ground settlement profiles fit well with the semi-empirical model proposed by Cham and Goh (2011).

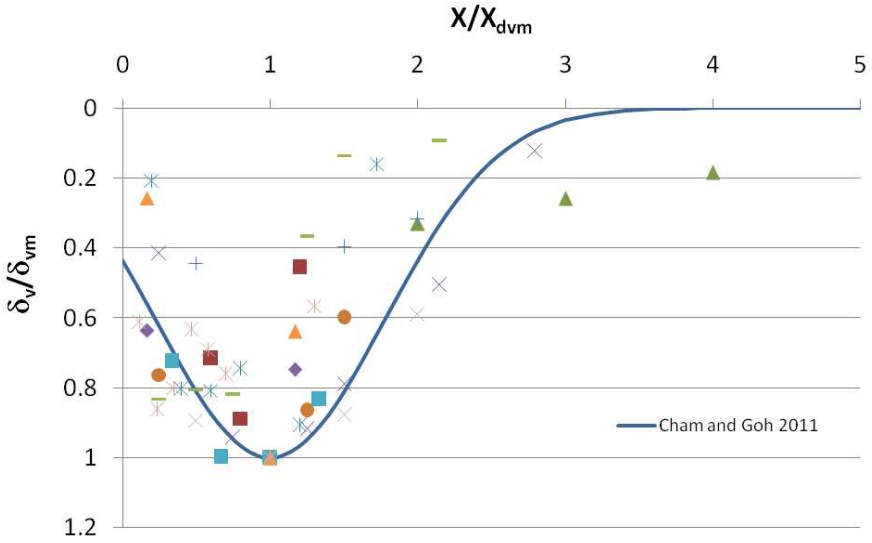


Figure 17. Normalized ground settlement profile based on Cham and Goh (2011)

CONCLUSION

This paper summarizes the general ground conditions, the excavation support system adopted, the construction activities and the field instrumentations for Cashew station. It then reviews the ground settlements, wall deflection profiles, strut loads, and ground water monitoring behavior. Generally, the diaphragm wall deflections are small, far below the alert level. The ground settlements are significant due to the considerable groundwater drawdown. In general, the ground settlements were smaller in locations where recharging was carried out, compared with those where recharging was not carried out. Comparisons of ground settlement profiles with empirical methods indicate that the ground settlement fits the pattern recommended by Peck (1969) and it also agrees well with the semi-empirical model proposed by Cham and Goh (2011). It is hoped that this case study will provide useful reference and insights for future projects involving excavation in the Bukit Timah Granite residual soils.

ACKNOWLEDGMENTS

The authors would like to acknowledge the financial support from LTIF project funded by the Land Transport Authority, Singapore. Special thanks are given to Dr Goh Kok Hun and Mr Otard Chew Yuen Sin of LTA for the helpful discussions and communications. In addition, the authors also thank LTA project manager Mr Soh Kin Meng (C913), deputy project manager Mr Kong Jian Yuan (C913), and Senior design manager Mr Chen Din Chong for their assistance in this project.

REFERENCES

Cham, W. M., and Goh, K. H. (2011). "Prediction of ground settlement due to adjacent deep excavation works." *Proc., Underground Singapore 2011*, NUS, Singapore, 94-103.

Lake, L. M., Rankin, W. J., and Hawley, J. (1996). *Prediction and effects of ground movements caused by tunneling in soft ground beneath urban areas*, Construction Industry Research and Information Association (CIRIA), London.

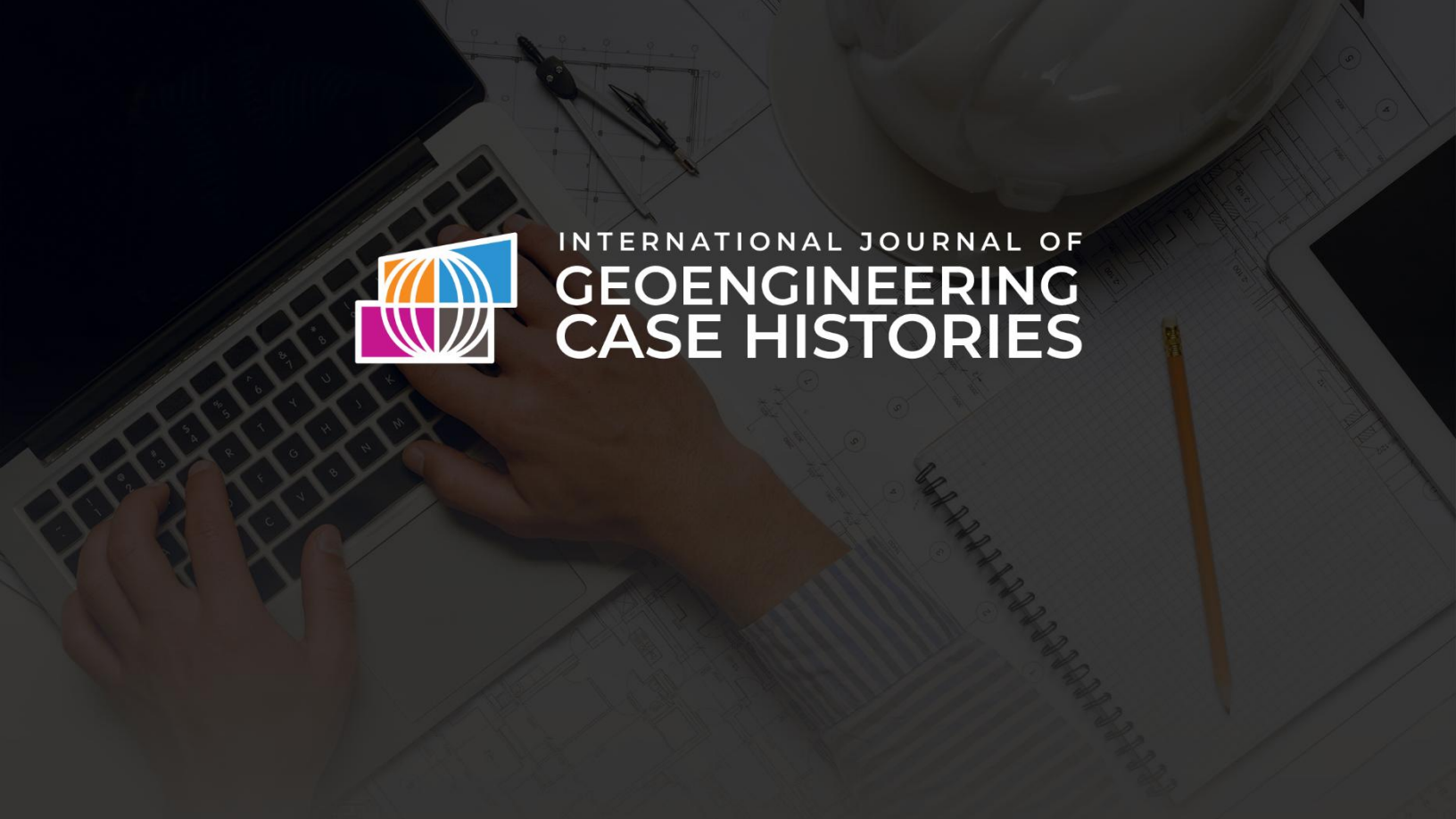
Clough, G. W., and O'Rourke, T. D. (1990). "Construction induced movements of in-situ walls." *Proc., Design and Performance of Earth Retaining Structure, Geotechnical Special Publication No. 25*, ASCE, New York, 439-470.

Hsieh, P. G., and Ou, C. Y. (1998). "Shape of ground surface settlement profiles caused by excavation." *Can. Geotech. J.,* 35(6), 1004-1017.

Ou, C. Y., Hsieh, P.G., and Chiou, D. C. (1993). "Characteristics of ground surface settlement during excavation." *Can. Geotech. J.*, 30(5), 758-767.

Peck, R. B. (1969). "Deep excavation and tunneling in soft ground." *Proc., 7th Int. Conf. on Soil Mechanics and Foundation Engineering*, Sociedad Mexicana de Mecanica, Mexico City, 225-290.

Terzaghi, K., and Peck, R. B. (1967). *Soil Mechanics in Engineering Practice*, 2nd Ed., Wiley, New York.



INTERNATIONAL JOURNAL OF
GEOENGINEERING
CASE HISTORIES

The Journal's Open Access Mission is generously supported by the following Organizations:

dar
a Sidara company

Geosyntec consultants
engineers | scientists | innovators

ConeTec

MUD BAY DRILLING
LANKELMA
Geotech DRILLING

ENGEO
Expect Excellence

Access the content of the ĪSSMGE Īnternational Journal of Geoengineering Case Histories at:
www.geocasehistoriesjournal.org

Downloaded: Thursday, November 19 2026, 08:40:57 UTC